IOCCG Protocol Series

Ocean Optics & Biogeochemistry Protocols for Satellite Ocean Colour Sensor Validation

Volume 2: Beam Transmission and Attenuation Coefficients: Instruments, Characterization, Field Measurements and Data Analysis Protocols (v2.0)

Authors
Emmanuel Boss, Michael Twardowski, David McKee, Ivona Cetinić and Wayne Slade

Editors
Aimee R. Neeley and Ivona Cetinić

International Ocean Colour Coordinating Group (IOCCG) in collaboration with National Aeronautics and Space Administration (NASA)

IOCCG, Dartmouth, Canada

April 2019

IOCCG Ocean Optics and Biogeochemistry Protocols for Satellite Ocean Colour Sensor Validation

IOCCG Protocol Series Volume 2.0, 2019

Beam Transmission and Attenuation Coefficients: Instruments, Characterization, Field Measurements and Data Analysis Protocols

Report of a NASA-sponsored workshop with contributions from:

Emmanuel Boss	University of Maine, Orono, ME, USA
Michael Twardowski	Harbor Branch Oceanographic Institute, Florida Atlantic University, FL, USA
David McKee	Physics Department, University of Strathclyde, Glasgow, Scotland, UK
Ivona Cetinić	NASA Goddard Space Flight Center, MD/ GESTAR Universities Space Research Association, MD, USA
Wayne Slade	Sequoia Scientific, Inc., 2700 Richards Road, Bellevue, WA, USA

Edited by:

Aimee R. Neeley and Ivona Cetinić

Correct citation for this volume:

IOCCG Protocol Series (2019). Beam Transmission and Attenuation Coefficients: Instruments, Characterization, Field Measurements and Data Analysis Protocols. Boss, E., Twardowski, M., McKee, D., Cetinić, I. and Slade, W. IOCCG Ocean Optics and Biogeochemistry Protocols for Satellite Ocean Colour Sensor Validation, Volume 2.0, edited by A. Neeley and I. Cetinić, IOCCG, Dartmouth, NS, Canada.
http://dx.doi.org/10.25607/OBP-458

Acknowledgements:

We thank the Editorial Review Board Members for their constructive comments on this document:

Giorgio Dall'Olmo	Plymouth Marine Laboratory (PML), UK
Toby K. Westberry	Oregon State University, OR, USA

http://www.ioccg.org

Published by the International Ocean Colour Coordinating Group (IOCCG), Dartmouth, NS, Canada, in conjunction with the National Aeronautics and Space Administration (NASA).

Doi: http://dx.doi.org/10.25607/OBP-458

Beam Transmission and Attenuation Coefficients: Instruments, Characterization, Field Measurements and Data Analysis Protocols

Emmanuel Boss[1], Michael Twardowski[2], David McKee[3], Ivona Cetinić[4,5] and Wayne Slade[6]

[1]*University of Maine, Orono, ME, 04469, USA*
[2]*Harbor Branch Oceanographic Institute, Florida Atlantic University, Fort Pierce, FL, USA*
[3]*Physics Department, University of Strathclyde, Glasgow, Scotland, UK*
[4]*NASA Goddard Space Flight Center, Code 616, Greenbelt, MD 20771, USA*
[5]*GESTAR/Universities Space Research Association, Columbia, MD 21046, USA*
[6]*Sequoia Scientific, Inc., 2700 Richards Road, Suite 107, Bellevue, WA, 98005, USA*

Introduction

Beam transmittance $T(\lambda, r_T)$ over an optical path of length r_T [m], and the beam attenuation coefficient $c(\lambda)$ [m^{-1}], are the probably the most used optical measurements in the field of oceanography. This document dives into the concepts behind the measurement, the instrumentation used for data collection, and analysis protocols to evaluate the same. The variables T and r_T are related by Eq. (6) in the following section. A beam transmissometer is an instrument that combines a source of collimated spectral radiant flux $\Phi_o(\lambda, 0,0,\bullet)$ and a co-aligned detector, to measure both the flux $\Phi_T(\lambda, r_T, 0,\bullet)$ transmitted over distance r_T and $T(\lambda, r_T)$ (Fig. 1 and related text in the following section). Beam transmissometers are also commonly known as beam attenuation meters or ac-meters.

Radiant flux transmission measurement concepts

Geometry and Nomenclature

In Fig. 1 the origin of a local instrument coordinate system is placed at the exit aperture of a source of monochromatic radiant flux $\Phi_o(\lambda, 0,0,0)$ [μW nm^{-1}]$\Phi_o(\lambda, 0,0,0)$ [in μW nm^{-1}][1] directed as a collimated beam along the positive z_m axis (see also Fig. 2.2 in Mueller and Morel 2003). The subscript "m" associated with the coordinate basis vectors $(\hat{\boldsymbol{x}}_m, \hat{\boldsymbol{y}}_m, \hat{\boldsymbol{z}}_m)$ in Fig. 1 indicates that the local "measurement" coordinate frame is associated with a particular instrument concept, as distinguished from global coordinates defining positions and directions in the extended medium (*cf* Figs. 2.1 and 2.2 in Mueller and Morel 2003). The local instrument coordinate framework is related to global coordinates by a translation and rotations that are arbitrary and need not be considered in the present context[2].

The direction associated with an optical path vector intersecting the transmitted beam axis (z_m axis) is described by the angle pair (ψ, ϕ), where $0 \le \psi \le \pi$ is measured from the z_m-axis and $0 \le \phi \le 2\pi$ is measured from the x_m-axis counterclockwise in the $x_m y_m$-plane. The variable *r*, with various subscripts, will denote geometric distance along any such optical path[3]. Directional radiant flux at distance *r* from a source, or from a scattering interaction site within the transmitted beam, is denoted $\Phi(\lambda, r, \psi, \phi)$. In Fig. 1 for example, radiometric flux scattered into direction (ψ, ϕ) at position x_s is denoted as $\Phi_S(\lambda, 0, \psi, \phi)$, and the scattered flux transmitted in that direction to Detector 2, at position x_D, as $\Phi_S(\lambda, r_D, \psi, \phi)$. Radiometric flux within the beam transmitted to a point on the z_m-axis at distance *r* from the source is denoted, $\Phi_T(\lambda, r, 0,\bullet)$,

[1] The choice of these units, rather than, e.g., W m^{-1}, is customary in ocean color science and is used throughout these protocols.

[2] When the IOP are used in the context of a radiative transfer model, on the other hand, the translations and rotations relating local coordinates, used to describe scattering interactions (e.g., as at position $\bar{\mathbf{x}}_S$ .in Fig. 1.3), to global coordinates, describing locations and directions in the medium as whole, become critically important.

[3] See Footnote 2 in Mueller and Morel (2003) regarding the usage of the variable *z* in Fig. 2.2 and Sect. 2.4 of Mueller and Morel 2003. Here we have substituted the symbol *r* for the optical pathlength along the z-axis in Fig. 1 (compare with Fig. 2.2 of Mueller and Morel 2003).

where the dot indicates that ϕ is indeterminate when $\psi = 0$ or $\psi = \pi$. In particular, the flux transmitted from the source to Detector 1 is $\Phi_T(\lambda, r_T, 0, \bullet)$.

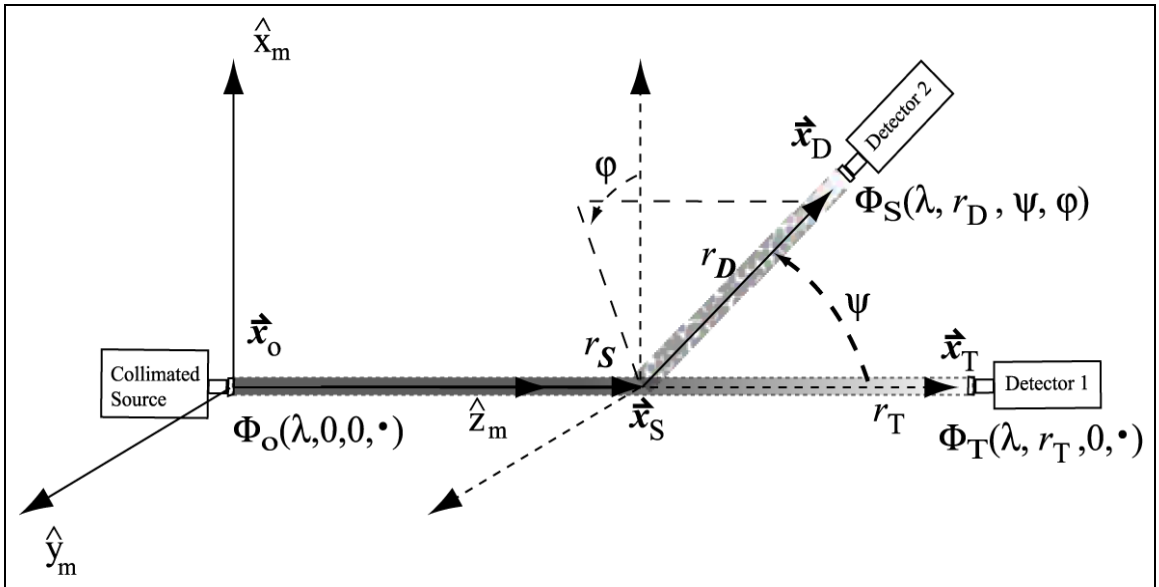

Figure 1: The local "Instrument Coordinate" framework describing optical beam transmission and scattering geometry. A collimated beam of radiometric flux $\Phi_o(\lambda, 0,0,\bullet)$ is emitted from a source at the origin $\vec{x}_o$. The flux within the collimated beam, shown schematically as a gradient shaded rectangle extending along the z_m-axis to Detector 1, is reduced by scattering and absorption as it is transmitted along the z_m-axis, and a reduced flux $\Phi_T(\lambda, r_T, 0,\bullet)$ is measured by Detector 1 at position $\vec{x}_T$. At the intermediate location $\vec{x}_S$, some fraction of the flux $\Phi_T(\lambda, r_S, 0,\bullet)$ that reaches that location is scattered out of the beam into direction (ψ, ϕ). The directionally scattered flux $\Phi_S(\lambda, 0, \psi, \phi)$ is subsequently transmitted a distance r_D in that direction, with further losses due to scattering and absorption, and the reduced scattered flux $\Phi_S(\lambda, r_D, \psi, \phi)$ is measured by Detector 2 at position $\vec{x}_D$. See text for further explanations. Modified after Pegau et al. (2003a).

Transmittance and Beam Attenuation

The shaded rectangle overlaid on the extended z_m axis in Fig. 1 schematically illustrates a cylinder (of cross-sectional area Δs) representing the collimated beam of radiant flux transmitted from the source to Detector 1. The gradient in shading represents the exponential decrease in $\Phi_T(\lambda, r, 0,\bullet)$ with increasing distance r, as photons interact with the medium and are absorbed and scattered out of the beam. During transmission over a path interval from r to $r + \Delta r$, the fraction of radiant flux absorbed in the volume $\Delta s \Delta r$ is spectral absorptance, and the fraction of flux scattered out of the beam direction in that volume is spectral scatterance (see Mueller and Morel 2003, Section 2.4).

One could envision superimposing a lightly shaded "cloud" on Fig. 1 to visualize scattered photons escaping from the beam in all directions, but this would not indicate the directional nature of the scattering losses. Instead, the scattering process is schematically illustrated in Fig. 1 as a mottled, shaded path of photons scattered in a particular direction (ψ, ϕ) at a single location $\vec{x}_S$ in the beam. At this on-axis location, x_s, similar beams could be drawn in any other direction to visually indicate scattered flux intensity and its subsequent transmittance and attenuation in the new direction. The same type of graphic could be drawn anywhere along the optical path; and if many were combined, the aforementioned "photon cloud" would be generated—masking any indication of the vector nature of the scattered radiant field. Nevertheless, that mental construct is adequate for considering transmission measurement concepts. If the pathlength r_T is short enough such that photons initially scattered out of the beam have a negligible chance of undergoing two (or more) additional scattering interactions that could return them to the beam, then it may be assumed that they will not be detected by Detector 1 (Fig. 1).

The beam attenuation coefficient is defined as

$$c(\lambda) = a(\lambda) + b(\lambda), \tag{1}$$

where the volume absorption and scattering coefficients $a(\lambda)$and $b(\lambda)$, both in [m^{-1}], are defined in terms of absorptance $A(\lambda)$ and scatterance $B(\lambda)$ in the limit of the optical pathlength Δr approaching zero as

$$a(\lambda) = \lim_{\Delta r \to 0} \frac{A(\lambda)}{\Delta r}, \text{and } b(\lambda) = \lim_{\Delta r \to 0} \frac{B(\lambda)}{\Delta r}, \tag{2}$$

respectively. Eq. (2.16) in Mueller and Morel (2003) may be rearranged as

$$\lim_{\Delta r \to 0} \left\{ \frac{\Phi_T(\lambda) - \Phi_i(\lambda)}{\Phi_i(\lambda) \Delta r} \right\} = \lim_{\Delta r \to 0} \left\{ -\frac{A(\lambda) + B(\lambda)}{\Delta r} \right\} \tag{3}$$

where Φ_i and Φ_T are incident and transmitted radiant fluxes, respectively. Eq. (3) may be expressed in differential form as

$$\frac{d\Phi(\lambda)}{\Phi(\lambda, r)} = -c(\lambda) dr \, . \tag{4}$$

Integrating Eq. (4) over an optical pathlength r_T as

$$c(\lambda) \int_0^{r_T} dr = -\int_0^{r_T} \frac{d\Phi(\lambda)}{\Phi(\lambda, r)}, \tag{5}$$

we obtain the solution for the beam attenuation coefficient

$$c(\lambda) = \frac{\ln \Phi_o(\lambda, 0, 0, \bullet) - \ln \Phi_T(\lambda, r_T, 0, \bullet)}{r_T} = \frac{-\ln T(\lambda, r_T)}{r_T}, \tag{6}$$

where we adopt the conventions and notations described above and in Fig. 1. In Eq. (6), transmittance $T(\lambda, r_T) \equiv \frac{\Phi_T(\lambda, r_T, 0, \bullet)}{\Phi_o(\lambda, 0, 0, \bullet)}$ is the fraction of radiant flux transmitted over the path distance r_T. Eq. (6) is the fundamental equation by which the beam attenuation coefficient is determined from a measurement made with a transmissometer.

The attenuation of radiant flux transmitted over a short optical pathlength r_T in seawater may be determined using the Beer-Lambert-Bouguer Law (Eq. 2.41 in Mueller and Morel 2003), which follows directly from Eq. (6) as

$$\Phi_T(\lambda, r_T, 0, \bullet) = \Phi_o(\lambda, 0, 0, \bullet) e^{-c(\lambda) r_T}. \tag{7}$$

Transmissometer Design Characteristics

In concept, a beam transmissometer is a relatively simple instrument to build, and the derived beam attenuation coefficient has a growing number of applications in ocean sciences (e.g., Boss et al. 2015). For that reason, instruments of this type have been in use for decades. While a great number of different transmissometer designs have appeared, most follow one of the two basic designs illustrated in Fig. 2.

Direct and folded path transmissometers

The most common transmissometer design uses a collimated light beam[4], with a source in one housing and a detector facing the source in another (Fig. 2, top). In such an ideal direct-path transmissometer, either a white light, or a light emitting diode (LED) of a specific wavelength, source is combined with a pinhole to provide a point source. A lens is inserted into the path to collimate the light beam; if needed, an interference filter is inserted to select the waveband of the measurement, and the light is passed into the water through a window. Other transmissometers (e.g., Sequoia's LISST[5]) use a laser source and a beam expander as a source. At the other end of the optical path, the light enters the detector assembly through another window and is focused by a lens. An aperture at the focal point removes off-axis scattered light, and the transmitted light falls on the detector. Although this instrument is conceptually simple, it is difficult to build. The alignment

[4] Cylindrically limited beam, as opposed to collimated beam, transmissometers will be discussed later in this section.

[5] Certain commercial equipment, instruments, or materials are identified in this chapter to foster understanding. Such identification does not imply recommendation, or endorsement, by the National Aeronautics and Space Administration, nor does it imply that the materials or equipment identified are necessarily the best available for the purpose.

of components is critical, and something as simple as the sagging of the filament in the source when the instrument is moved can create significant apparent changes in the derived beam attenuation coefficient.

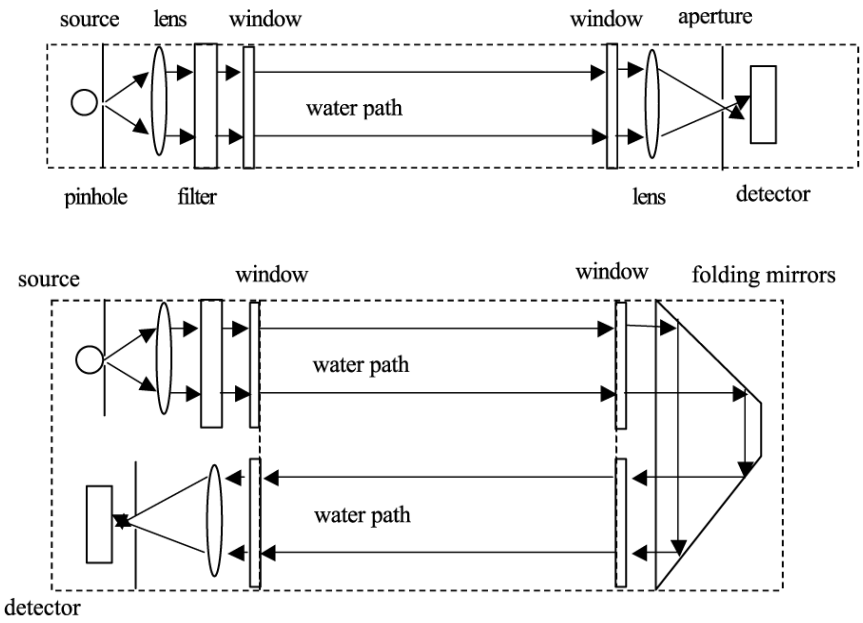

Figure 2. Schematic illustrations of direct path (top panel) and folded path (bottom panel) beam transmissometers designs.

Several commercial transmissometers including some laboratory spectrophotometers and the (former) SeaTech and Sea-Bird Scientific (Bellevue, WA, USA; formerly WET Labs Inc.) field instruments use this basic design. Design variations include the addition of a reference detector and placing the wavelength filter in the detector housing.

Other types of transmissometers

The folded-path transmissometer pathlength design uses one or more reflectors to create a longer pathlength. The basic idea for this design can be attributed to Petterson (1934). Initial designs used plane mirrors to expand the pathlength (Wattenberg 1938; Timofeeva 1960). The introduction of prisms to separate the incident and reflected beam (Nikolayev and Zhil'tsov 1968; Petzold and Austin 1968) and of concave mirrors as the reflectors, have led to improved versions of this general design. An optical pathlength of 10 m was achieved by Jerlov (1957) by using multiple reflections between three concave mirrors. Long pathlength instruments of this type are specifically beneficial for measurements of beam attenuation coefficient in clear, open ocean waters.

A variable pathlength transmissometer is probably the most desirable, and elusive, design concept. One desirable characteristic of such a transmissometer would be its capability to adjust the pathlength for the measuring conditions (see *Pathlength Considerations*, below). More importantly, the variable pathlength instrument would be self-calibrating. To understand this property of such an instrument, examine the basic Eq. (6) for transmissometer measurements. For any transmissometer measurement over pathlength r_i, the dark-corrected detector output $V_T(\lambda, r_i)$, in [V], is proportional to the flux reaching the detector window $\Phi_T(\lambda, r_i, 0, \bullet)$. If two transmissometer measurements are made using different path lengths, r_1 and r_2, the transmittance over the pathlength difference between the two measurements is simply

$$T(\lambda, r_2 - r_1) \equiv \frac{\Phi_T(\lambda, r_2, 0, \bullet)}{\Phi_T(\lambda, r_1, 0, \bullet)} = \frac{V_T(\lambda, r_2)}{V_T(\lambda, r_1)}, \tag{8}$$

and the beam attenuation coefficient $c(\lambda)$ may be calculated from Eq. (6) with $r_T = r_2 - r_1$. The assumptions implicit in this calculation are that the beam attenuation coefficient is constant over the time and space extents

of the measurements, and that the optical alignment and electronic properties of the instrument also are constant over time.

Barth et al. (1997) describe the design and application of a variable pathlength instrument for use in coastal waters. However, they also note that the errors in alignment made their instrument unsuitable for clear water applications. The requirement to exactly repeat the optical alignment at two distances is the most difficult aspect of building a variable pathlength instrument. Small changes in the alignment of the reference detector, or reflector, will introduce large errors in the beam attenuation coefficient by causing the focal point of the beam to wander relative to the aperture in front of the detector. If biofouling exists, the spatial gradients in the fouling will cause $V_T(\lambda, r_i)$ to vary if the alignment is not perfect. Additionally, if the beam is not truly collimated, but instead has a slight divergence, the beam divergence will cause a different area of the detector window to be illuminated in each measurement, and any spatial gradients in the optical properties of the window will translate into errors in $c(\lambda)$.

Many laboratory benchtop spectrophotometers have a design very similar to a collimated beam transmissometer. A complication that arises when using laboratory spectrophotometers to measure beam attenuation is that much of the scattered light is kept in the sample by the total-internal-reflection at the glass-air interface. This makes it more likely that multiply scattered light will be received at the detector. This problem can be reduced by the addition of light baffles within the sample cuvette. In addition, such spectrophotometers have a large, and often unknown, acceptance angle at the receiver end (see below).

Source and detector characteristics

The transmittance ratio $\frac{\Phi_T(\lambda,r_T,0,\bullet)}{\Phi_o(\lambda,0,0,\bullet)}$, i.e., the ratio of the flux transmitted to the detector window divided by the flux entering the water at the source window, must be known to compute $c(\lambda)$ from Eq. (6). A transmissometer does not actually measure either of these quantities. A transmissometer's detector output signal $V_D(\lambda)$ represents its response in the presence of flux $\Phi_D(\lambda)$, the part of $\Phi_T(\lambda, r_T, 0,\bullet)$ that arrives at the detector after passing through the instrument's detector assembly window and other optical elements (Fig. 2). Because of reflections and absorption during transmission through windows and other optical components $\Phi_T(\lambda, r_T, 0,\bullet) > \Phi_D(\lambda)$, but assuming the optical throughput is linear, $\Phi_T(\lambda, r_T, 0,\bullet) \propto \Phi_D(\lambda)$. The detector's "dark" response $V_D^{\text{dark}}(\lambda)$ is any signal output that is present when the source is off and $\Phi_T(\lambda, r_i, 0,\bullet) = 0$. If the detector's electrical response is linear, $\Phi_D(\lambda) \propto \left[V_D(\lambda) - V_D^{\text{dark}}(\lambda)\right]$ and may be written as

$$\Phi_T(\lambda, r_T, 0,\bullet) = C_D\left[V_D(\lambda) - V_D^{\text{dark}}(\lambda)\right], \tag{9}$$

where C_D is a constant, with units of [W nm$^{-1}V^{-1}$], accounting for the combined effects of optical losses and the detector's flux responsivity.

A measure of the flux $\Phi_o(\lambda, 0_i, 0,\bullet)$ is still required if the transmission is to be determined. A beam splitter before the source window can be used to shunt a proportion of the source light to a reference detector to provide a measure of the flux being sent into the water. Because of losses associated with the source windows and beam splitter, the reference detector receives and responds to a flux proportional to $\Phi_o(\lambda, 0_i, 0,\bullet)$, such that

$$\Phi_o(\lambda, 0,0,\bullet) = C_R\left[V_R(\lambda) - V_R^{\text{dark}}(\lambda)\right], \tag{10}$$

where $V_R(\lambda)$ and $V_R^{\text{dark}}(\lambda)$ are the reference detector response and ambient (dark) signals, respectively, and C_R is a second system response constant.

The transmittance may now be written as the ratio of Eq. (9) and Eq. (10)

$$T(\lambda, r_T) = \frac{\Phi_T(\lambda,r_T,0,\bullet)}{\Phi_o(\lambda,0,0,\bullet)} = C_T\,\frac{\left[V_D(\lambda) - V_D^{\text{dark}}(\lambda)\right]}{\left[V_R(\lambda) - V_R^{\text{dark}}(\lambda)\right]}, \tag{11}$$

where $C_T = \frac{C_D}{C_R}$.

If the source output is constant, the constant $\left[V_R(\lambda) - V_R^{\text{dark}}(\lambda)\right]$ may be absorbed in C_T and Eq. (11) reduces to

$$T(\lambda, r_T) = \frac{\Phi_T(\lambda, r_T, 0, \bullet)}{\Phi_o(\lambda, 0, 0, \bullet)} = C_T\left[V_D(\lambda) - V_D^{\text{dark}}(\lambda)\right], \quad (12)$$

and there is no need to use a reference detector[6] output to calculate transmittance.

Depending on a transmissometer's design, we must determine the coefficient C_T in either Eq. (11) or Eq. (12). It is not practical to determine the system response constants based on first principles because they are dependent on the optical component throughputs, the combined responses of the detectors, and electronic circuits. Instead, a system's calibration constant C_T (dimensionless in Eq. 11, or in V^{-1} in Eq. 12) is typically determined by measuring the instrument's output in a "standard" medium having a known beam attenuation coefficient $c_{\text{STD}}(\lambda)$. For oceanographic transmissometers, the "standard" medium is highly purified water (See *Characterization and Calibration* section below), and $c_{\text{STD}}(\lambda) = c_w(\lambda)$ (see Section 1.2 in Pegau et al. 2003a). Note, however, that in some cases, filtered seawater or purified water with added salts may provide a better blank. This will be the case if the particulate beam attenuation is sought (e.g., Slade et al. 2010) or when the water body investigated has such a high concentration of dissolved salts as to significantly impact the transmission between the water and source windows (Boss et al. 2013a).

Transmissometer Response Temperature Dependence

The source output, responsivity of the detector, and performance of other electronic components tend to be temperature dependent. This causes the calibration constants to be temperature dependent. Two approaches are used to remove the temperature dependence: 1) add compensating electronics that allow the voltage output to remain constant over a temperature range, or 2) measure the temperature of the instrument and determine the how the constants change with temperature. The first technique is used in many single-wavelength transmissometers, such as the Sea Tech and Sea-Bird Scientific transmissometers. The second approach is used in the Sea-Bird Scientific ac-9 and ac-s spectral absorption and beam attenuation meters.

Spectral Characteristics

Many areas of research in ocean optics require knowledge of the spectral beam attenuation coefficient $c(\lambda)$. Several transmissometers have been built to provide this spectral information. Matlack (1974) used an instrument with a grating monochromator to measure $c(\lambda)$ in the wavelength range from 385 nm to 565 nm. Using a pair of circular wedge interference filters, Lundgren (1975) was able to measure the beam attenuation coefficient at wavelengths between 340 nm and 730 nm. More recent transmissometers that use a monochromator as the detector include the one described by Barth et al. (1997). Sabbah et al. (2010) built a transmissometer with 2-nm spectral resolution from 300 nm to 750 nm using two light sources and two spectrometers. Another design for obtaining the spectral beam attenuation coefficient utilizes several interference filters mounted in a wheel that rotates through the beam. Examples of filter-wheel transmissometer designs include the VLST (Petzold and Austin 1968) and the Sea-Bird Scientific ac-9 (Moore et al. 1992; Van Zee et al. 2002).

Bandwidth considerations

Bandwidth matters in measurements of beam attenuation. If the bandwidth is too wide, Beer's law does not apply. An example showing it is as follows: assume a source with bandwidth Δλ, with a light source whose intensity that is not a function of wavelength, measuring in a medium where the beam attenuation is a linear function of wavelength, e.g., $c(\lambda) = c_0 + \delta\lambda$.

The attenuation of the beam's energy will follow:

$$\mathrm{I(r)} = \frac{\mathrm{I_0}}{\Delta\lambda}\int_{-\frac{\Delta\lambda}{2}}^{\frac{\Delta\lambda}{2}} \exp(-\mathrm{c}(\lambda)\mathrm{r})\mathrm{d}\lambda = \frac{\mathrm{I_0}\exp(-\mathrm{c_0 r})}{\Delta\lambda}\int_{-\frac{\Delta\lambda}{2}}^{\frac{\Delta\lambda}{2}} \exp(-\delta\lambda)\mathrm{d}\lambda = \mathrm{I_0}\exp(-\mathrm{c_0 r})\frac{\sinh(\delta\Delta\lambda \mathrm{r})}{\delta\Delta\lambda \mathrm{r}}$$
$$\xrightarrow{\Delta\lambda \to 0} \mathrm{I_0}\exp(-\mathrm{c_0 r})\left(1 + \frac{(\delta\Delta\lambda \mathrm{r})^2}{6}\right) \quad (13)$$

[6] A reference detector may be used in a feedback circuit to stabilize an LED source. However, the reference detector signal is not usually included in the instrument's data output stream in constant source output designs of this type.

where the term in the bracket represent the first two terms of the Taylor expansion. Hence, the longer the pathlength (r), the larger the deviation from a constant value (δ); or the larger the bandwidth (Δλ), the more divergent the measured attenuation will be from the spectrally averaged attenuation—and, in addition, Beer's law will not be observed (the decrease of intensity with distance will not be exactly exponential).

Beam geometry, detector acceptance angle and scattered light

Real transmissometers do not have perfectly collimated sources or detectors. Unlike the idealized detector concept of Fig. 1, a detector with a finite acceptance angle, or field of view (FOV) ψ_{FOV}, detects photons that are singly scattered in the range $0 < \psi \leq \psi_{\mathrm{FOV}}$. Therefore, the flux $\Phi_T^M(\lambda, r_T, 0, \bullet)$ arriving at a transmissometer's detector assembly window and subsequently measured (see above) exceeds the true flux directly transmitted along the path direction $\psi \equiv 0$ according to

$$\Phi_T^M(\lambda, r_T, 0, \bullet) = \Phi_T(\lambda, r_T, 0, \bullet) + 2\pi \int_0^{\psi_{\mathrm{FOV}}} \beta(\lambda, \psi, \phi)\, sin\, \psi\, d\psi, \tag{14}$$

where $\beta(\lambda, \psi, \phi)$ is the volume-scattering function (VSF), in units of [m^{-1} sr^{-1}] (Section 1.5 in Pegau et al. 2003a). In other words, because a transmissometer measures a portion of the forward scattered light, its measurement overestimates the transmittance $T(\lambda, r_T)$ and underestimates the beam attenuation coefficient calculated with Eq. (6). The acceptance angle, and thus the scattering error, is dependent on the optical elements of the instrument. There is no standard specified for transmissometer acceptance angle, and each manufacturer may use a different one for each particular instrument design (e.g., Table 1 in Boss et al. 2009). Therefore, were the transmittance of a homogeneous water volume to be measured by a number of perfectly calibrated beam attenuation meters (from Sequoia Scientific, Sea-Bird Scientific, or Sea Tech, for example), each instrument model would yield a different $c(\lambda)$, because of its different acceptance angle. These differences also depend on the shape of VSF. Indeed, Boss et al. (2009), observed such differences between four different commercial transmissometers, and their differences were explained by the variation in the near-forward part of the VSF.

These considerations lead to two questions: 1) What is the best detector acceptance-angle choice for a transmissometer design? 2) What method should be used to correct the beam attenuation measurements for scattered light acceptance?

The first question appears to have a simple answer. The above discussion and Eq. (14) would seem to imply that the smaller the acceptance angle, the better the measurement. That may not be correct. One must further consider what is being measured when choosing the acceptance angle (Pegau et al. 1995), and particularly at very small angles, in the presence of near-forward scattering. Density fluctuations due to natural, or instrument related, turbulence steer the beam into random fluctuations and increase the apparent beam attenuation coefficient (Bogucki et al. 1998, Mikkelsen et al. 2008) independently from ordinary molecular- and particle-scattering processes (Section 1.5 in Pegau et al. 2003a). How might this phenomenon affect a particular application of the measurement? If interested in inverting the spectral beam attenuation coefficient to determine particle properties, a beam attenuation meter that is particularly sensitive to scattering by turbulence would not be a good choice. On the other hand, for active LIDAR imaging systems, it may be important to know the transmittance effects due to very-near-forward scattering independent of the sources that may dominate the scattering process. From another perspective, the angular resolution of radiative transfer models tends to be larger than one degree, so fine angular resolution of the volume scattering coefficient and related beam attenuation coefficient is not needed for accurate model calculations (Mobley et al. 1993). For many such calculations. it is preferable to smooth the highly forward-peaked phase function (Fig. 1.3 in Pegau et al. 2003a; Pegau et al. 2003b) and decrease the beam attenuation coefficient accordingly. Gordon (1993) indicates that, for irradiance-level radiative transfer, it is possible to completely disregard scattering in the first 15°, an angle much larger than the acceptance angles of transmissometers. Finally, from an engineering perspective, it is more difficult to build a stable transmissometer with a very small acceptance angle. Based on these considerations, most transmissometers are designed with an acceptance angle $\lesssim 1°$.

The second question has been addressed by several investigators over the years (Gumprecht and Sliepcevich 1953; Jones and Wills 1956; Jerlov 1957; Duntley 1963; Voss and Austin, 1993). Voss and Austin (1993) examined the scattering error for both collimated beam and cylindrically limited instruments designs. They found that the percent error increases with increasing acceptance angle and with increasing $c(\lambda)$. They predicted an average error for a 670-nm transmissometer with a 1.0° acceptance angle of

approximately 19% (though differences as high as 100% were observed by Boss et al., 2009 and McKee et al., 2013). Accurate correction of an apparent $c_M(\lambda)$ measured by that instrument would require knowing both the VSF $\beta(\lambda,\psi,\phi)$ over the range $0 < \psi \leq \psi_{\mathrm{FOV}}$ and the single scattering albedo $\omega_o(\lambda) = \frac{b(\lambda)}{c(\lambda)}$ (Section 2.4 in Mueller and Morel 2003). The former could be provided from laser *in situ* scattering and transmissometry (LISST) measurements (Slade et al. 2006). However, given the extreme rate of increase in the magnitude of the VSF for particles $\beta_p(\lambda,\psi,\phi)$, its large variability in the environment, and the potential contribution of turbulence, as $\psi \to 0$ (Fig. 1.3 in Pegau et al. 2003a), any estimate of its integrated value over the range $0 < \psi \leq 1°$ would be highly uncertain. That uncertainty would transmit directly into any $c(\lambda)$ correction algorithm attempting to account for the effects of the near-forward VSF.

One approach to dealing with the effects of scattered light in measured beam attenuation coefficients is that proposed by both Voss and Austin (1993) and Pegau et al. (1995). That is, do not try to apply any scattering corrections to the measured determination of $c(\lambda)$. Simply report the acceptance angle characteristics of the transmissometer used to make the measurements and leave all considerations of how to handle scattering artifacts to the user of the data. Internal consistency of IOP is obtained by including light scattered up to a certain acceptance angle ψ_{FOV} in the beam attenuation coefficient, and not including it in the VSF. We may rewrite Eq. (1), $c(\lambda) = a(\lambda) + b(\lambda)$, as

$$c(\lambda) = a(\lambda) + 2\pi \int_{\psi_{\mathrm{FOV}}}^{\pi} \beta\,(\lambda,\psi)\, sin\,\psi\, d\psi + 2\pi \int_{0}^{\psi_{\mathrm{FOV}}} \beta\,(\lambda,\psi)\, sin\,\psi\, d\psi, \tag{15}$$

or,

$$c_m(\lambda) = c(\lambda) - 2\pi \int_{0}^{\psi_{\mathrm{FOV}}} \beta\,(\lambda,\psi)\, sin\,\psi\, d\psi = a(\lambda) + 2\pi \int_{\psi_{\mathrm{FOV}}}^{\pi} \beta\,(\lambda,\psi)\, sin\,\psi\, d\psi = a(\lambda) + b_m(\lambda) \tag{16}$$

where $c_m(\lambda)$ and $b_m(\lambda)$ are the measured beam attenuation and volume scattering coefficients, respectively. This approach, which has been most commonly adopted and is likely to remain so in the near future, leaves the uncomfortable problem of different sensors providing different attenuation values—varying by as much as a factor of two or more. In an attempt to address this, McKee et al. (2013) presented an iterative scattering-correction method for Sea-Bird Scientific ac-9 and ac-s data that corrects both absorption and attenuation measurements. The technique requires additional backscattering data to facilitate estimation of particulate backscattering ratios that enable selection of error estimates based on previous Monte Carlo simulations of the attenuation sensor. The technique avoids the difficulty of direct measurement of forward-scattering VSFs that can be influenced by turbulence and provides an estimate of corrected attenuation that is relevant for studies focused on particle scattering. At the time of writing, only very limited validation data has been available, but initial results demonstrated that there was strong consistency with LISST attenuation data, overcoming the significant differences in scattering collection angles (~0.93° vs ~0.027° in water). As the prevalence of data sets featuring both attenuation and VSF measurements grows, the potential exists to establish mutually consistent estimates of attenuation due to water, particles, and dissolved materials. However, this will require considerable further effort before a recommendation can be made. An unambiguous measurement of attenuation, free from scattering-error artifacts, remains elusive and consideration of alternative approaches to this problem by the community should be encouraged.

In another design variant, the beam is cylindrically limited rather than collimated. In the cylindrically limited light arrangement, the pinhole at the source is imaged on the receiver lens, and the receiver aperture is focused on the source lens. This design illuminates a large volume of water and uses more of the source light. No currently available commercial instruments use the cylindrically limited design, although at one point in history, transmissometers of this type were manufactured by Martek. The Visibility Laboratory Spectral Transmissometer (VLST) was a laboratory-built instrument using a cylindrically limited beam in a folded-path configuration (Petzold and Austin 1968). Several copies of the VLST, built in the late 1970's, continued in use to measure $c(\lambda)$ until *circa* 1990.

Pathlength considerations

The theoretical interpretation of transmissometer data assumes a single-scattering regime, that is, the detector does not collect photon that have scattered multiple times. According to van de Hulst (1981), this translates to a requirement that the pathlength be approximately the reciprocal of the beam attenuation measured, e.g. *r ~ 1/c*. A pathlength that is too short will result in a low signal-to-noise ratio (small changes

in intensity for large changes in c) while a pathlength that is too long will be biased low because the photons collected will have experienced multiple scattering events.

The $r \sim 1/c$ requirement, however, ignores several important aspects of the measurement: 1) absorption does not contribute to scattering (rather acts preferentially on multiply scattered photons due to their increased pathlength); and 2) the VSF of oceanic particles is highly peaked in the forward direction, such that a large number of scattered photons are collected into the detector and, hence, do not count as scattered photons.

In an absorbing-only medium, attenuation and absorption are equal, and the only consideration regarding pathlength would be that sufficient signal reaches the receiver such that the uncertainty due to receiver sensitivity is low. In this case, the absolute uncertainty in absorption can be shown to equal the relative uncertainty of the signal measured at the detector, e.g. $|\delta a| \sim \frac{1}{r}\left|\frac{\delta I}{I}\right|$. Hence, both increased pathlength and increased signal are desired (which are contradictory), with increased sensitivity (δI) providing an independent trade-space to decrease uncertainty (e.g. allowing for measurements in more absorbing waters with an instrument of a pathlength > $1/a$).

The same exact argument is applicable for the effective attenuation in the single-scatter regime $|\delta c| \sim \frac{1}{r}\left|\frac{\delta I}{I}\right|$. In most ocean waters, multiple-scattered light is not, in general, a problem for the commercially available transmissometers. If scattered light leaves the beam then it will take two additional scattering events to bounce the light back into the beam and redirected towards the detector. The addition of baffles along the light path can nearly eliminate any possibility of multiply scattered light being detected in ordinary circumstance. Indeed, Monte-Carlo simulations of beam transmissometers (Piskozub et al. 2004 and Leymarie et al. 2010) suggest that, for realistic VSF and typical oceanic and coastal water conditions, multiple scattering is not a big factor. For a 0.25-m pathlength transmissometer with an acceptance angle of 0.93° and a beam attenuation of 100 m^{-1}, the deviation of the measured attenuation from the bias due to multiple scattering events is on the order of 30% (Leymarie et al. 2010).

There are also engineering concerns associated with the optical pathlength. The path must be short enough that light reaches the detector; there is no benefit to an instrument with a path length $r_T \approx 10c(\lambda)^{-1}$ m, because the transmitted signal would not be detectable. On the other hand, the pathlength must be long enough for attenuation to reduce the transmitted flux enough that the difference in incident and transmitted fluxes are large enough to be measurable. Longer pathlengths also reduce the relative uncertainty in the measurement of the pathlength r_T.

A pathlength in the range $c(\lambda)^{-1} \leq r_T \leq 3c(\lambda)^{-1}$ is generally considered close to optimal. As electronics and sources have improved, however, instruments with pathlengths $r_T < c(\lambda)^{-1}$ $r_T < c(\lambda)$ m^{-1} have been shown to work well over a wide range of oceanic conditions.

Ambient light rejection in open and enclosed path transmissometers

Basic transmissometer designs (Fig. 2) do not physically reject all ambient sunlight, which could add to the measured flux (though for a well-collimated detector, this is unlikely). Enclosed path designs that place the optical path within a cell through which the water is pumped, such as the ac-9, block more ambient light physically but are not totally immune to its effects. Some scheme must be developed to remove ambient light artifacts. A simple approach is to measure the signal with the source on and with the source off. The ambient signal with the source off is used as the dark reference for relating output signal to transmitted flux. The current generation of instruments use a more sophisticated, but similar, approach. The light source is rapidly modulated (chopped), and the detector output is phase-locked to the modulation frequency so that the transmitted flux is proportional to the amplitude of the alternating component of detector output. The key underlying assumption is that the natural light field varies slowly and is not part of the alternating signal. This approach may have difficulties when the ambient light also varies rapidly, such as with indoor lights that have inherent 60-Hz fluctuation or near the ocean surface where waves may rapidly modulate the light field. Even with good electronic rejection of ambient light, it is wise to reduce the possible influence of ambient light by using baffles and carefully positioning the instrument.

Characterization and Calibration of Beam Transmissometers

Calibration with pure water

As explained above, the calibration constant C_T for a transmissometer is determined by measuring its response to a "standard" medium having a known value of $c_{\mathrm{STD}}(\lambda)$. The optical "standard" medium commonly used to calibrate oceanographic transmissometers and absorption meters (Twardowski et al. 2018b) is pure water, so that $c_{\mathrm{STD}}(\lambda) = c_w(\lambda) = a_w(\lambda) + b_w(\lambda)$. The recommended values of $a_w(\lambda)$ are taken from Table 1.1 in Twardowski et al. (2018a), and $b_w(\lambda)$ from Table 1.1 in Pegau et al. (2003a).

Pure water of optical calibration grade is freshly prepared by methods described in Twardowski et al. (2018b). This difficult step is critical because residual traces of particles and/or dissolved organic material introduce serious calibration offsets and relative uncertainties between calibrations. The pure water standard is introduced into the optical path by one of two methods:

1. An open path transmissometer must be thoroughly cleaned and rinsed in purified water, and then immersed in a test tank containing the pure water standard. Care must be taken to prevent bubbles from collecting on the instrument's optical windows. It is ordinarily not practical to carry out this calibration procedure at sea.
2. To calibrate an enclosed path instrument, a volume of the pure water standard is pumped through the flow-through measurement cell, as described in detail in Twardowski et al. (2018b) for the ac-9, as an example. Procedures to assure bubbles do not form within, or be introduced into, the flow-through measurement cell (Twardowski et al. 2018b) must be followed carefully. This pure-water calibration procedure can be carried out at sea, and it is recommended to do so daily, whenever possible.
3. In general, sensors should be calibrated in the same orientation and strapped to the platform to which they will be attached. This insures that the calibration accounts for small alignment changes that may occur.

In either case, after allowing suitable time for the instrument to warm up, the instrument signal outputs in response to flux transmitted in the pure water standard and dark (ambient) background, $V_{\mathrm{D,w}}(\lambda)$ and $V_{\mathrm{D,w}}^{\mathrm{dark}}(\lambda)V_{\mathrm{D,w}}(\lambda)$ and $V_{\mathrm{D,w}}^{\mathrm{dark}}(\lambda)$ (and if appropriate, also $V_{\mathrm{R,w}}(\lambda)$ and $V_{\mathrm{R,w}}^{\mathrm{dark}}(\lambda)V_{\mathrm{R,w}}(\lambda)$ and $V_{\mathrm{R,w}}^{\mathrm{dark}}(\lambda)$), are recorded over a several minute sampling period and averaged.

For pure water, the forward scattering is sufficiently small such that the acceptance angle has little effect on the calibration. From Eq. (7), the transmittance of the pure water standard is $T_w(\lambda, r_T) = e^{-c_w(\lambda)r_T}$. For an instrument with a source reference detector, substitute from Eq. (11) to write

$$C_T(\lambda) = T_W(\lambda, r_T)\frac{\left[V_{\mathrm{R,w}}(\lambda) - V_{\mathrm{R,w}}^{\mathrm{dark}}(\lambda)\right]}{\left[V_{\mathrm{D,w}}(\lambda) - V_{\mathrm{D,w}}^{\mathrm{dark}}(\lambda)\right]}, \tag{17}$$

or for an instrument with a constant source output, substitute from Eq. (12) to write

$$C_T(\lambda) = \frac{T_W(\lambda, r_T)}{\left[V_{\mathrm{D,w}}(\lambda) - V_{\mathrm{D,w}}^{\mathrm{dark}}(\lambda)\right]}, \tag{18}$$

as appropriate.

By straightforward combinations of Eqs. (6), (11) and (17) it is easy to show that for a transmissometer with a source reference detector,

$$T(\lambda, r_T) = T_W(\lambda, r_T)\frac{\left[V_{\mathrm{R,w}}(\lambda) - V_{\mathrm{R,w}}^{\mathrm{dark}}(\lambda)\right]}{\left[V_{\mathrm{D,w}}(\lambda) - V_{\mathrm{D,w}}^{\mathrm{dark}}(\lambda)\right]}\frac{\left[V_D(\lambda) - V_D^{\mathrm{dark}}(\lambda)\right]}{\left[V_R(\lambda) - V_R^{\mathrm{dark}}(\lambda)\right]}, \text{ and}$$

$$c(\lambda) - c_w(\lambda) = \frac{-1}{r_T} ln\left\{\frac{\left[V_{\mathrm{R,w}}(\lambda) - V_{\mathrm{R,w}}^{\mathrm{dark}}(\lambda)\right]}{\left[V_{\mathrm{D,w}}(\lambda) - V_{\mathrm{D,w}}^{\mathrm{dark}}(\lambda)\right]}\frac{\left[V_D(\lambda) - V_D^{\mathrm{dark}}(\lambda)\right]}{\left[V_R(\lambda) - V_R^{\mathrm{dark}}(\lambda)\right]}\right\} \tag{19}$$

or combining Eqs. (6), (12) and (18) for a transmissometer with a constant source output

$$T(\lambda, r_T) = T_W(\lambda, r_T)\frac{\left[V_D(\lambda) - V_D^{\mathrm{dark}}(\lambda)\right]}{\left[V_{\mathrm{D,w}}(\lambda) - V_{\mathrm{D,w}}^{\mathrm{dark}}(\lambda)\right]}, \text{ and}$$

$$c(\lambda) - c_w(\lambda) = \frac{-1}{r_T} ln\left\{\frac{\left[V_D(\lambda) - V_D^{\mathrm{dark}}(\lambda)\right]}{\left[V_{\mathrm{D,w}}(\lambda) - V_{\mathrm{D,w}}^{\mathrm{dark}}(\lambda)\right]}\right\}. \quad (20)$$

The essential calibration factors to be reported, therefore, are the detector response and ambient (dark) offset in pure water $V_{\mathrm{D,w}}(\lambda)$ and $V_{\mathrm{D,w}}^{\mathrm{dark}}(\lambda)$, as well as the response and ambient offset $V_{\mathrm{R,w}}(\lambda)$ and $V_{\mathrm{R,w}}^{\mathrm{dark}}(\lambda)$ of a source reference detector (if applicable). The total beam attenuation coefficient, $c(\lambda)$, may be easily determined by adding $c_w(\lambda)$ from Table 1.1 in Pegau et al. 2003a to the difference calculated with Eq. (19) or (20).

An alternative approach to determining the total beam attenuation coefficient directly from the measured voltage response is to determine, from the pure water calibration, a calculated offset reference voltage $V_{\mathrm{ref}}(\lambda)$ and dark offset $V_{\mathrm{dark}}(\lambda)$such that the total transmittance may be calculated directly as

$$T(\lambda, r_T) = \frac{\left[V_D(\lambda) - V_{\mathrm{D,w}}^{\mathrm{dark}}(\lambda)\right]}{\left[V_{\mathrm{ref}}(\lambda) - V_{\mathrm{D,w}}^{\mathrm{dark}}(\lambda)\right]}, \quad (21)$$

where it is assumed that $V_D^{\mathrm{dark}}(\lambda) = V_{\mathrm{D,w}}^{\mathrm{dark}}(\lambda)$ varies very slowly over time and may be treated as an instrument constant. This approach is only used with transmissometers assumed to have a constant source output, examples of which include the former SeaTech red transmissometers. The value of $V_{\mathrm{ref}}(\lambda)$ is calculated by combining Eq. (21) with the transmittance relationship in Eq. (20) as

$$T(\lambda, r_T) = T_W(\lambda, r_T)\frac{\left[V_D(\lambda) - V_D^{\mathrm{dark}}(\lambda)\right]}{\left[V_{\mathrm{D,w}}(\lambda) - V_{\mathrm{D,w}}^{\mathrm{dark}}(\lambda)\right]} = \frac{\left[V_D(\lambda) - V_{\mathrm{D,w}}^{\mathrm{dark}}(\lambda)\right]}{\left[V_{\mathrm{ref}}(\lambda) - V_{\mathrm{D,w}}^{\mathrm{dark}}(\lambda)\right]}, \quad (22)$$

from which it easily follows that

$$V_{\mathrm{ref}}(\lambda) = \frac{V_{\mathrm{D,w}}(\lambda) - V_{\mathrm{D,w}}^{\mathrm{dark}}(\lambda)}{T_W(\lambda, r_T)} + V_{\mathrm{D,w}}^{\mathrm{dark}}(\lambda). \quad (23)$$

The SeaTech transmissometers were calibrated to read $c_w(650) = 0.364$ m^{-1} in pure water. This approach perhaps simplifies the determination of $c(\lambda)$ for the inexperienced user, but at the same time obscures the value of $c_w(\lambda)$ used to determine the offset reference voltage.

Air calibration

Only in cases where it is impossible to perform clean water calibrations, is it advisable to do air calibration, as the latter can result in significant offset uncertainties.

The sensors output signal response $V_{\mathrm{D,air}}^{f}$and dark offset $V_{\mathrm{D,air}}^{\mathrm{dark,f}}$are recorded in air by the manufacturer at the time of each factory's water calibration. These values are typically reported with the calibration records, as "factory" air calibration and dark values (and thus the superscript "f"), to allow the user to periodically record "air calibration" or "air tracking" data as a check on instrument stability. Air tracking is primarily intended to be used to monitor offsets in the instrument's output due to changes in the optical system caused by shipping or mounting of the instrument to a cage or other deployment package. Air tracking can also be used to monitor instrument drift over extended periods of time. Historically, before the advent of pure water field calibrations, the air calibration was the only stability tracking method available.

Air tracking data is best obtained in the laboratory, where the environment is consistently clean and dry, preferably before and after each transmissometer deployment. Although air calibrations can be performed while in the field, it is—at best—difficult to do them on a ship due to the moist environment. Readings in air may be significantly offset by small amounts of moisture either condensed on or adsorbed in the windows.

Detailed protocols for carrying out air calibrations are provided for particular instruments by the manufacturer. In general terms, the protocols include instructions and methods for the careful cleaning of optical surfaces, allowing time for exposed optical surfaces to dehydrate in a dry environment, and procedures to avoid or compensate for temperature increases when the instrument is operated in air.

Using air-calibration values, user can adjust the transmission measured in the field following (Gardner et al. 2017):

$$T^{adjusted} = T(\lambda, r_t)\frac{V^{f}_{\mathrm{D,air}}}{V_{D,air}}, \quad (24)$$

where the dark offset voltage measured in factory and field are assumed negligible. If the manufacturer instead provides a factory reference voltage for calibrating the instrument using Eq. (21), the adjusted pure water and dark values should be substituted in Eq. (23) to determine $V_{\mathrm{ref}}^{\mathrm{adjusted}}$. Air calibration adjustments of this type are usually recommended only for instruments with "constant" LED source output, such as the Sea-Bird Scientific C-Star, older SeaTech red transmissometers, and other similar instruments by different manufacturers. Field water calibrations are the recommended basis for correcting drifts in closed-path, flow-through cell instrument, such as the ac-9 and ac-s.

There are instances where water calibration is impractical (e.g. transmissometers on UNOLS vessel do not get calibrated regularly). In such cases researchers often will use Eq. 24 and additionally will remove from each profile the clearest value in a deep cast (Gardner, 2019, personal communication). The bias in such cases, for open ocean waters at 1000 m, is on the order of 0.01 m^{-1} at 660 nm (Boss et al. 2015).

Instrument temperature dependence

The change in a transmissometer's response and dark values are usually determined by measuring response variations with the optical path in air, or in a dry, inert gas such as nitrogen or argon, as the instrument temperature varies. The response and dark values at each internal instrument temperature (an ancillary measurement and data output needed for temperature corrections) are recorded and reported either as a lookup table of correction factor and temperature pairs, or as the coefficients of a polynomial function of temperature that has been fit to the correction factors. Instruments that have a closed, flow-through optical cell are usually characterized in a water bath—the temperature of which is cycled over a range typically from 5 °C to 30 °C over the course of the experiment. To avoid condensation, the flow-through cell is usually filled with a dry, inert gas and sealed. The internal instrument temperatures are somewhat higher than the ambient temperature, due to heating by the electronic circuits and source. If this experiment is done with air in the optical path of an open-path transmissometer, i.e., in a temperature-controlled chamber, some method must be used and documented to avoid artifacts due to condensation on the windows.

Field Measurement Methods

The procedures for measuring *in situ* profiles, over depth z, of $c(z, \lambda)$ using constant output LED source transmissometers are straightforward. The instrument is connected to a data acquisition system and mounted on a profiling cage following the manufacturer's instructions (e.g., avoid torquing the optical path in CStar transmissometer). If the instrument has an analog output, the user must ensure that the external analog-to-digital converter used to digitize the readings is calibrated in absolute units of electric potential [Volts], since that is the basis on which the instrument has been calibrated.

The windows on the beam transmissometer must be cleaned using the following procedure: 1) wipe the optical windows with a lens paper moistened with a mild detergent solution 2) using a squirt bottle, rinse with distilled water to remove the detergent 3) wipe the optical windows with another lens paper moistened with isopropyl alcohol 4) rinse with with distilled water, and, finally, 5) remove excess moisture from the optical windows using a dry lens paper. An air check reading could be made before every cast to verify that the windows are clean. A transmissometer dark voltage should also be measured at this time. These on-deck air calibrations should be logged and compared to the more careful air calibrations done under dry laboratory conditions before and after each cruise (see the *Characterization and Calibration* section). If pre- and post-cruise air calibrations are significantly different, the time history should indicate whether the change occurred suddenly (e.g*.,* a scratch in the window) or as a drift over time.

Each time an open-path transmissometer is placed into the water, care must be taken to assure that bubbles do not collect on the windows, particularly if the instrument is mounted in a vertical orientation.

Protocols covering methods for making field measurements with the ac-9 and ac-s instruments are described in detail in Zee et al. (2002) and Sullivan et al. (2006) respectively. Some critical aspects of these protocols are briefly reviewed in Twardowski et al. (2018b) to emphasize their importance.

Multi- and hyperspectral transmissometers, that can be deployed with flow-sleeves, should be deployed with a 0.2-μm filter on the intake several times in a field campaign. The simple shape of the CDOM spectra

provides a check on the calibration used and, in addition if using an ac-9 or ac-s, a cross calibration with the a-side of the instrument.

For long-term deployments, pre- and post-calibration should be made, with care to keep the sensors damp, or wet with local water until post-calibration can take place (without cleaning the instrument before the calibration). Such post-calibration should be done within short period post recovery preventing the additional growth on optical windows. Another calibration after cleaning should take place to assess the effect of fouling relative to instrumental drift.

Data Analysis Methods

There are several generic steps needed to process and analyze a vertical profile of measured transmissometer data:

1. Merge the transmissometer data with externally-measured depth and temperature data. Assuming that the transmissometer does not have an internal, high-quality depth transducer, it is usually mounted together with a CTD to provide the depth and water temperature fields.
2. For instruments that are deployed in closed-path configuration (e.g., flow-through mode, or aboard a cage where water is fed by a pump), apply lag corrections to account for the time interval between when water enters the intake port and when it enters the beam attenuation measurement optical path in a flow-through transmissometer. For the configurations where velocity of the water is not known, calculation of the delay can be done either with a flow meter, or other simple measurement of the water velocity.
3. Subtract the depth offset between the pressure transducer used to measure package depth and either
    a. The intake port of a flow-through transmissometer, or
    b. The midpoint of the optical path in an open path transmissometer.
4. Field calibration adjustments should be applied by the methods specified by the manufacturer of a particular instrument. In many cases this will involve entering the changes in an instrument calibration file used by the computer software that implements and applies Eq. (19) or (20) to calibrate the data.
    a. Pure water calibration results are the preferred source of these adjustments for flow-through instruments.
    b. Air calibration for tracking drift corrections should be applied using only data from calibrations carried out under dry laboratory conditions and showing insignificant variations between replicated calibrations. When the manufacturer represents the calibration coefficients in terms of a reference signal to be applied using Eq. (21), the corrected air calibration factor is computed using Eq. (24).
5. Instrument internal temperature compensation factors should be applied in the manner specified by the manufacturer of a particular instrument.
6. Compute transmittances $T(\lambda, r_T)$, and beam attenuation coefficients $c(\lambda) - c_w(\lambda)$ offsets, relative to pure water using the appropriate combination of Eqs. (19), (20) or (21) with Eq. (6) for the instrument type and output data.
7. For measurements in the red and near-infrared, compute temperature offsets due to difference in water temperature between reference and *in situ* measurement. Apply temperature offset following the method of Sullivan et al. 2006.
8. Add pure water $c_w(\lambda)$, determined from Table 1.1 in Pegau et al. (2003a) to $c(\lambda) - c_w(\lambda)$ to obtain the total beam attenuation coefficient $c(\lambda)$.
9. Despite best efforts, it is sometime impossible to obtain accurate enough calibration for long cruises to obtain stable values at deep clear waters. A practical solution has been to use air reference (Eq. 24) and further adjust the beam attenuation by removing from the profile its minimal value in a deep cast.

Detailed procedures required to carry out each of the above steps for particular instrument are typically provided by the manufacturer. Sea-Bird Scientific., for example, provides both a User's Manual for its ac-9 and ac-s absorption and beam attenuation coefficient meter, and a detailed ac-9 and ac-s Protocol Manual (Van Zee et al. 2002); additional information from the latter document, regarding absorption and beam attenuation measurements, is outlined in Twardowski et al. (2018b) and Pegau et al. (2003c).

Many of the steps listed above also apply when a transmissometer is installed and operated on a ship as a component of an along-track measurement system. The lengthy plumbing path in such a system introduces intake-to-measurement lags of up to several minutes, while a research vessel typically advances approximately one kilometer in three minutes. Therefore, accurate temporal and spatial co-registration of, e.g., surface water temperature, chlorophyll *a* fluorescence, and $c(\lambda)$ requires accurate determination of the flow rate and lag time between a water volume's intake (usually in a ship's sea chest), passage through some debubbler apparatus, and arrival in the measurement cell of each instrument. The addition of an automated switch that periodically diverts the flow through a filter with a 0.2 μm pore size, provides calibration-independent measurements of the particulate beam attenuation (Slade et al. 2010), as long as the filtered attenuation is sampled at appropriate frequencies. Periodic cleaning of in-line instruments (e.g. at least once per week or more in high-productivity waters, e.g., Boss et al. 2013b) is critical to obtain high-quality data.

REFERENCES

Barth, H., K. Grisard, K. Holtsch, R. Reuter, and U. Stute, 1997. Polycromatic transmissometer for *in situ* measurements of suspended particles and gelbstoff in water. *Appl. Opt.*, **36(30):** 7919-7928.

Bogucki, D.J., J.A. Domaradzki, D. Stramski and J.R.V. Zaneveld, 1998. Comparison of near-forward light scattering on oceanic turbulence and particles. *Appl. Opt.*, **37(21):** 4669-4677.

Boss, E., W.H. Slade, M. Behrenfeld, and G. Dall'Olmo, 2009: Acceptance angle effects on the beam attenuation in the ocean. *Opt. Exp.*, **17(3)**: 1535-1550.

Boss, E., H. Gildor, W. Slade, L. Sokoletsky, A. Oren, and J. Loftin, 2013a: Optical properties of the Dead Sea. *J. Geophys. Res.*, **118,** doi:10.1002/jgrc.20109.

Boss, E., M. Picheral, T. Leeuw, A. Chase, E. Karsenti, G. Gorsky, L. Taylor, W. Slade, J. Ras, and H. Claustre, 2013b: The characteristics of particulate absorption, scattering and attenuation coefficients in the surface ocean; Contribution of the Tara Oceans expedition. *Meth. Oceanogr*., http://dx.doi.org/10.1016/j.mio.2013.11.002.

Boss, E., L. Guidi, M. J. Richardson, L. Stemmann, W. Gardner, J. K. B. Bishop, R. F Anderson, R. M Sherrell, 2015: Optical techniques for remote and in-situ characterization of particles pertinent to GEOTRACES. *Prog. Ocean.*, **133:** 43-54,

Duntley, S.Q., 1963. Light in the sea. *J. Opt. Soc. Amer*., 53(2): 214-233.

Gardner, W. D., B. E. Tucholke, M. J. Richardson, P. E. Biscaye, 2017: Benthic storms, nepheloid layers, and linkage with upper ocean dynamics in the western North Atlantic. *Mar. Geol.*, 385, 304-327.

Gordon, H.R., 1993. Sensitivity of radiative transfer to small-angle scattering in the ocean: Quantitative assessment. *Appl. Opt*., **32(36):** 7505-7511.

Gumprecht, R.O. and C.M. Sliepcevich, 1953: Scattering of light by large spherical particles. *J. Opt. Soc. Am.*, **57:** 90-94.

Jerlov, N.G., 1957: A transparency-meter for ocean water, *Tellus*, **9**: 229-233.

Jones, D. and M.S. Wills, 1956: The attenuation of light in sea and estuarine waters in relation to the concentration of suspended solid matter. *J Mar. Biol. Assoc. U.K*., **35:** 431-444.

Kitchen, J.C., J.R.V. Zaneveld and H. Pak, 1982: Effect of particle size distribution and chlorophyll content on beam attenuation spectra. *Appl. Opt*. **21**: 3913-3918.

Leymarie, E., D. Doxaran, and M. Babin, 2010: Uncertainties associated to measurements of inherent optical properties in natural waters. *Appl. Opt*, **49**: 5415-5436.

Lundgren, B., 1975: Measurements in the Baltic with a spectral transmittance meter. *Univ. Copenhagen, Inst. Phys. Oceanogr. Rep.*, **30:** 28pp.

Matlack, D.E., 1974: Deep ocean optical measurements (DOM) report on North Atlantic, Caribbean, and Mediterranean cruises. *Tech. Rep. Naval Ordnance Lab.*, pp 1-103.

McKee, D., J. Piskozub, R. Röttgers, and R. A. Reynolds, 2013: Evaluation and improvement of an iterative scattering correction scheme for in situ absorption and attenuation measurements. *J. Atmos. Oceanic Tech.*, **30**: 1527-1541.

Mikkelsen, O. A., T. G. Milligan, P. S. Hill, R. J. Chant, C. F. Jago, S. E. Jones, V. Krivtsov, and G. Mitchelson-Jacob, 2008: The influence of schlieren on in situ optical measurements used for particle characterization. *Limnol. Ocean. Meth.*, **6**:133-143

Moore, C., J.R.V. Zaneveld and J.C. Kitchen, 1992: Preliminary results from an *in situ* spectral absorption meter. *Ocean Optics XI*, *Proc. SPIE* **1750:** 330-337.

Mobley, C.D., and OTHERS, 1993. Comparison of numerical models for computing underwater light fields. *Appl. Opt.*, **32(36):** 7484-7504

Mueller, J.L. and A. Morel (2003), Fundamental Definitions, Relationships and Conventions, in *Ocean Optics Protocols for Satellite Ocean Color Sensor Validation, Revision, Volume I: Introduction, Background and Conventions*, NASA/TM-2003-21621/Rev4-Vol. I, edited by J.L. Mueller, G.S. Fargion, and C.R. McClain, pp. 11-29, NASA Goddard Space Flight Center, Greenbelt, Maryland.

Nikolayev, V.P. and A.A. Zhil'tsov, 1968: Simple photoelectric transparency meter. *Oceanology (U.S.S.R.)*, **8:** 428-432.

Pegau, W. S., J. R. V. Zaneveld, and K. J. Voss, 1995: Toward closure of the inherent optical properties of natural waters. *J. Geophys. Res.*, **100:** 13,193-13.

Pegau, S., R.V. Zanevled and J.L. Mueller (2003a), Inherent Optical Property Measurement Concepts: Physical Principles and Instruments, in *Ocean Optics Protocols for Satellite Ocean Color Sensor Validation, Revision 4, Volume IV: Inherent Optical Properties: Instruments, Characterizations, Field Measurements and Data Analysis Protocols,* NASA/TM-2003-211621/Rev4-Vol. IV, edited by J.L. Mueller, G.S. Fargion, and C.R. McClain, pp. 1-14, NASA Goddard Space Flight Center, Greenbelt, Maryland.

Pegau, S., R.V. Zanevled and J.L. Mueller (2003b), Beam Transmission and Attenuation Coefficients: Instruments, Characterization, Field Measurements and Data Analysis Protocols, in *Ocean Optics Protocols for Satellite Ocean Color Sensor Validation, Revision 4, Volume IV: Inherent Optical Property Measurement Concepts: Physical Principles and Instruments*, NASA/TM-2003-211621/Rev4-Vol. IV, edited by J.L. Mueller, G.S. Fargion, and C.R. McClain, pp. 15-26, NASA Goddard Space Flight Center, Greenbelt, Maryland.

Pegau, S., R.V. Zanevled and J.L. Mueller (2003c), Volume Absorption Coefficients: Instruments, Characterization, Field Measurements and Protocols, in *Ocean Optics Protocols for Satellite Ocean Color Sensor Validation, Revision 4, Volume IV: Inherent Optical Property Measurement Concepts: Physical Principles and Instruments*, NASA/TM-2003-211621/Rev4-Vol. IV, edited by J.L. Mueller, G.S. Fargion, and C.R. McClain, pp. 27-38, NASA Goddard Space Flight Center, Greenbelt, Maryland.

Pettersson, H., 1934: A transparency-meter for sea-water. Medd. Oceanogr. Inst. Gothenberg, Ser. B **4**.

Petzold, T. and R.W. Austin, 19686: An underwater transmissometer for ocean survey work, In: *Underwater Photo-optical Instrument Applications*, Proc. SPIE 12: 133-137.

Piskozub, J., D. Stramski, E. Terrill, and W. K. Melville, 2004: Influence of forward and multiple light scatter on the measurement of beam attenuation in highly scattering marine environments. *Appl. Opt.*, **43**: 4723-4731.

Reynolds, R. A., D. Stramski, V. M. Wright, and S. B. Woźniak. 2010: Measurements and characterization of particle size distributions in coastal waters. *J. Geophys. Res*, **115**: C08024

Sabbah, S., J.M. Fraser, E.S. Boss, I. Blum, and C.W. Hawryshyn, 2010: Hyperspectral portable beam transmissometer for the ultraviolet-visible spectrum. *Limnol. Oceanogr.: Methods* **8:** 527-538.

Slade, W.H. and E. Boss, 2006: Calibrated Near-Forward Volume Scattering Function Obtained from the LISST Particle Sizer. *Opt. Expr.*, **14(8)**: 3602-3615.

Slade, W.H, E. Boss, G. Dall'Olmo, M.R. Langner, J. Loftin, M.J. Behrenfeld, C. Roesler, and T.K. Westberry, 2010: Underway and moored methods for improving accuracy in measurement of spectral particulate absorption and attenuation. *J. Atmos. Ocean. Tech.*, **27(10**): 1733-1746.

Sullivan, J.M., M.S. Twardowski, J.R.V. Zaneveld, C. Moore, A. Barnard, P. Donaghay, and B. Rhoades. 2006. The hyperspectral temperature and salinity dependencies of absorption by water and heavy water in the 400-750 nm spectral range. *Appl. Opt.,* **45**:5294-5309.

Timofeeva, V.A., 1960: Instrument for determining the attenuation coefficient of directed light in the sea. *Sov. Oceanogr. 1962 Ser.*, **4:** 79-83.

Twardowski, M., R. Röttgers and D. Stramski (2018a), The Absorption Coefficient, in Inherent Optical Property Measurements and Protocols: Absorption Coefficient, Neeley, A.R. (ed.), *IOCCG Ocean*

Optics and Biogeochemistry Protocols for Satellite Ocean Colour Sensor Validation, Volume 1.0, pp. 1-17, IOCCG, Dartmouth, NS, Canada.

Twardowski, M., R. Röttgers and D. Stramski (2018b), Reflective Tube Absorption Meters, in Inherent Optical Property Measurements and Protocols: Absorption Coefficient, Neeley, A.R. (ed.), *IOCCG Ocean Optics and Biogeochemistry Protocols for Satellite Ocean Colour Sensor Validation*, Volume 1.0, pp. 18-36, IOCCG, Dartmouth, NS, Canada.

Van Zee, H., D. Hankins, and C. deLespinasse, 2002: *ac-9 Protocol Document (Revision F)*. WET Labs Inc., Philomath, OR, 41pp.

Voss, K.J. and R.W. Austin, 1993. Beam-attenuation measurement error due to small-angle scattering acceptance. *J. Atmos. and Oceanic Tech*., **19(1):** 113-121

Wattenberg, H., 1938: Untersuchungen uber Durchsichtigkeit und Farbe des Seewassers, I. *Kieler Meeresforsch*., **2**.